Integrated three-dimensional modeling approach of stacked turbidite channels

Richard Labourdette

ABSTRACT

Hydrocarbon fields consisting of turbidite deposits are commonly more complex than anticipated because of fine-scale sedimentary heterogeneities, which complicate the reservoir characteristics. This is particularly evident in turbiditic channel complexes with lateral channel migration.

The creation of fine-scale models is founded on high-resolution seismic data, incorporating all available data together with concepts of the internal reservoir architecture. The model is essential for understanding the impact of these phenomena on reservoir characteristic distributions. The lateral extents and a real distribution of heterogeneity are still unknown; thus, our modeling workflow is incorporated into an uncertainty chain to identify and measure all uncertainties with a possible effect on static connectivity.

Internal channel complex fill is composed of multiple individual (elementary) channel stacks formed during repeated erosion-deposition cycles. These elementary structures allow sand transport through deep-sea areas and the preservation of slumps and slides on channel borders, resulting in the formation of internal heterogeneities. The sideways and downdip movement of elementary channels in turbidite complexes show two typical channel patterns: lateral migration and vertical stacking. The spatial distribution of slide heterogeneities is therefore constrained by the different channel patterns. Distinguishing between these two patterns provides an understanding of heterogeneity distributions and the resulting differences in static connectivity. These contrasts can be explained as distinct preservation rates of mass-transport slide sediments within elementary channels and can thus be included in reservoir models to define preferential zones of heterogeneity preservation along turbidite complexes.

Manuscript received December 12, 2006; provisional acceptance April 19, 2007; revised manuscript received May 30, 2007; final acceptance June 21, 2007.
DOI:10.1306/06210706143

AUTHOR

Richard Labourdette ~ *Structural Geology, Sedimentology and Geology Laboratory, TOTAL S.A., Pau, France; richard.labourdette@total.com*

Richard Labourdette has 15 years of experience in the petroleum industry and has been involved in the three-dimensional sedimentary modeling project of Total since 1993. He received his M.Sc. degree in reservoir geology and is currently finishing his Ph.D. (Montpellier University). His main focus is the sedimentary modeling of reservoirs and analog outcrops. He is part of the European Association of Geoscientists and Engineers Distinguished Lecturer Program (2005, 2006, and 2007).

ACKNOWLEDGEMENTS

I thank Eduardo Remacha, Philippe Crumeyrolle, Jean-Loup Rubino, Martine Bez, François Temple, Carlos Pirmez, William McCaffrey, Colin P. North, Roger M. Slatt, and Arthur H. Saller for their discussions and contributions relating to the evolution of sinuous turbidite channels and manuscript improvement and Pierre Biver for his help on uncertainty management. I also thank Sociedade Nacional de Combustíveis de Angola (SONANGOL), Esso Exploration Angola (Block 17) Ltd., BP Exploration (Angola) Ltd., Statoil Angola Block 17 A.S., Norsk Hydro, and Total for permission to present the information contained in this article.

INTRODUCTION

Many reservoirs encountered in deep-offshore continental-margin settings are large, erosionally confined, deep-water channel complexes; a spectrum of architectural styles and channel-fill types are observed (Abreu et al., 2003). Most of these large, sand-rich channel complexes contain sand-prone intervals associated with highly sinuous channel elements. Improved technology has enabled several workers to report deep-water channels with various degrees of sinuosity in modern deep-water fans (e.g., Garrison et al., 1982; Damuth et al., 1983, 1988). Their significance in subsurface exploration has only recently been assessed and has been improved by three-dimensional (3-D) seismic technology and ever-increasing deep-water exploration activities in offshore areas (Stephens et al., 1996; Kolla et al., 2001).

The highly sinuous channel forms identified in the subsurface range in complexity according to the number of laterally and vertically stacked depositional events (Kolla et al., 1998; Posamentier and Kolla, 2003). These channels form viable exploration targets (Roberts and Compani, 1996; Stephens et al., 1996).

Internal channel architecture, which is not clearly imaged in low-resolution seismic data (35 Hz), can now be recognized and mapped in detail using high-resolution (approximately 65 Hz) 3-D seismic data. Multiattribute interpretation of seismic facies has led to the definition of architectural elements as constituent parts of reservoir architecture. These elements are characterized by consistent sedimentological bodies such as erosive channels, channel margins, and stacked channels with higher or lower degrees of aggradation, and by lateral migration (Kolla et al., 2001; Posamentier and Kolla, 2003). They are calibrated by wells, characterized by petrophysics, and used to fill reservoir models. Even if small-scale heterogeneities are now well understood and modeled from outcrop analogs (Tomasso et al., 2006; Van Dyke et al., 2006; Slatt et al., in press), classical subsurface reservoir models commonly focus on external architectural element distributions commonly resulting in a limited rendering of associated internal heterogeneity (Stright et al., 2006; Weimer and Slatt, 2007). This approximate result means an incomplete assessment of reservoir compartmentalization and, therefore, reduced control of hydrocarbon recovery.

New data set acquisition during development of confined deep-water channel complex reservoirs (complementary wells, four-dimensional high-resolution seismic data, and production history) shows differences between initial reservoir models and subsequent observations. Inspection of logs and cores shows the presence of smaller scale bedding within seismically defined architectural elements (Prather et al., 2000). New interpretations have highlighted the importance of sedimentary heterogeneities such as shale barriers and channel baffles (Kolla et al., 2001) that cannot be mapped with conventional seismic data and, therefore, remain subseismic.

To avoid complications when matching well tests and production history, it is crucial to incorporate heterogeneity more precisely in the early geomodels. This need is apparent because water and gas breakthrough occurred earlier and at higher rates than predicted by earlier reservoir models.

Integrating high-resolution seismic data, well information, outcrop analog observations, and well production history with evolving computer performance now allows the identification and modeling of features that correspond to reasonable sand-body geometries. The modeling workflow can now be effectively carried out at scales excluding statistical downscaling processes (Hurst et al., 2000). These processes were previously necessary to distribute fine-scale heterogeneities in reservoir models. However, this type of model can favor upscaling of the petrophysical properties to be included in the final full-field model. Because of its fine-scale definition, it could also be used to test dynamic simulations (Labourdette et al., 2006) or invert deposit parameters conforming production statistics in accordance with seismic attributes.

The sinuous channels studied are Oligocene in age and are from the Malembo Formation of the Tertiary Congo Fan, seaward from the paleoshelf margin in the upper channel-levee system. This study focuses specifically on the terminal part of channel complex infill, where the channels are unconfined (or only very broadly confined), exhibit the single-cycle seismic character, and where individual channels are very clearly resolved (Mayall and Stewart, 2000).

Sand systems were generally deposited at sequence boundaries in cut-and-fill channels, which commonly exhibit internal meandering geometries and variable net-to-gross sand, both vertically and laterally (Da Costa et al., 2001; Posamentier and Kolla, 2003).

By describing the morphological and infill characteristics of a relatively simple but sinuous channel form in some detail, the main heterogeneities can be identified. These heterogeneities are then modeled by integrating the observations, concepts, and uncertainties and thereby assessing their impact on static connectivity.

DESCRIPTION OF THE CHANNEL MIGRATION

General Description

Submarine channels are known to follow moderately sinuous courses (Menard, 1955). Mutti and Normark (1991) use the term ''turbidite channel'' to refer to a long-term conduit for sediment to be transported downslope or at slope to base-of-slope settings. This term is not applied to the degree of erosion or confinement. Confined channels in particular are elongated, negative relief features produced by downcutting of turbidity currents (E. Mutti, 1992, personal communication). The term ''erosionally confined channel'' is used here to define deep-water channels in which confinement is mostly caused by erosion of older deposits; only coeval levee deposits may be partially preserved (Abreu et al., 2003). Erosionally confined channels commonly have a degradation profile in cross section and are distinct from aggradational channels where confinement is mostly caused by levee-building processes (Skene et al., 2002; Abreu et al., 2003).

In many recent studies involving side-scan sonar images, multibeam bathymetry, high-resolution seismic data, and coring and drilling in recent years, sinuous channel forms are described as common depositional elements of recent deep-sea fans fed by mud-rich terrigenous sediment sources (Garrison et al., 1982; Damuth et al., 1983, 1988; Kolla and Coumes, 1987; Beaubouef, 2004; Saller et al., 2004). Outcrop studies have confirmed their occurrence in various depositional settings, associated with diverse sediment infill, from mud-rich to sand-rich sediment sources, and from passive to active margin settings (e.g., Cronin, 1995; Elliott, 2000; Martinsen et al., 2000; Prather et al., 2000; Weimer et al., 2000; Young et al., 2003; Arnott, 2005). The depositional and erosional characteristics of these and other associated forms are now integrated into most turbidite-focused research.

Despite the high variability of channel complex infill (sand content from 20 to 70%), a general model was described by Mayall and Stewart (2000). Our study focuses on the last member of the channel complex infill, where the channels are either unconfined or only confined in very broad terms. They form the single-cycle seismic character, and individual channels can be very clearly identified (Mayall and Stewart, 2000). This last member of the channel infill is the most heterogeneous reservoir in hydrocarbon development potential of individual channel systems. The final phase of the channel complex infill is a generally lower net-to-gross sequence deposited by a highly sinuous channel-levee system (Mayall and Stewart, 2000; Mayall and O'Byrne, 2002).

Seismic Characterization

In the example described, seismic data used are part of a 54-fold, 3-D grid with bin size of 12.5 × 12.5 m (41 × 41 ft), covering an area of 13,000 km^2 (5019 mi^2) offshore Angola. The methodology divides the channel images seen in 3-D seismic data into several intervals, subsequently displayed as amplitude attribute maps. The following description is based on 65-Hz 3-D seismic data calibrated by 21 wells and 60 m (196.85 ft) of cores.

High-resolution 3-D seismic data allow internal channel architectures to be recognized and mapped in detail. Amplitude extractions and horizon slices in the upper erosional channel-fill sequence (Figure 1a) display a moderate- to high-sinuosity channel as Abreu et al. (2003) describe. Meanders evolve, migrate, and are commonly cut off throughout deposition just like those of subaerial meandering rivers (Damuth et al., 1988; Nelson and Smith, 1989; Mayall and Stewart, 2000). The main difference is aggradational and downdip components, which are visible in the seismic section of Figure 1b and suggest that deposition commonly involves longitudinal (downslope) migration or meander sweep accompanied by increased channel sinuosity through time (Kastens and Shor, 1985; Stelting et al., 1985; Coterill et al., 1999; Peakall et al., 2000; Kolla et al., 2001; Abreu et al., 2003; Posamentier and Kolla, 2003; Temple and Broucke, 2004). In such a migration, two typical channel organizations can be distinguished within the same channel complex, i.e., true lateral-migration and vertically stacked pattern configurations (Figure 1b).

The lateral-migration configuration is typically characterized by bright amplitudes on the inner bends with a scroll bar pattern in map view, associated with shingled reflections observed on vertical seismic profiles (Figure 1c, d). In general, the shingled reflections are parallel to the inside bend of the last position of the channel fill (Mayall and Stewart, 2000; Abreu et al., 2003). Shingled reflections geometry shows clearly defined patterns (Figure 1a, d) parallel to the channel margin and dipping toward the channel along which they formed.

Each inclined seismic reflection is interpreted as the position of the inner bank of the channel during migration. Shingled reflection packages represent the record

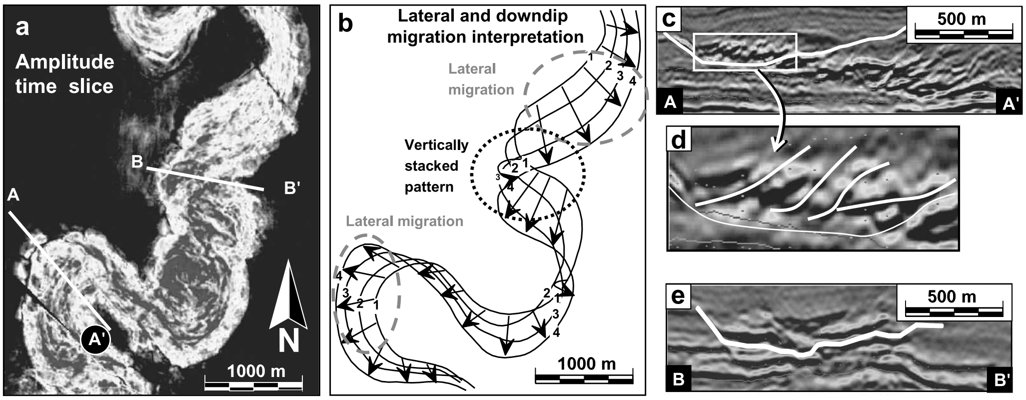

Figure 1. Seismic characterization of lateral migration. (a) Amplitude map in the lateral offset stacked channels. (b) Lateral- and downdip migration interpretation of the amplitude time slice, with channel center lines distinguishing lateral-migration and vertically stacked patterns. (c) Seismic section in the true lateral-migration area showing the accretionary organization of shingled beds (AA′). (d) Close-up of the morphology of shingled reflections. (e) Seismic section in the vertically stacked pattern (BB′).

of the lateral and downdip channel migration, with each reflection corresponding to accretionary beds deposited on the inner channel bends (Abreu et al., 2003).

The vertically stacked pattern configuration is defined by subhorizontal seismic reflections in section view (Figure 1b), with no scroll bar pattern in map view. Abreu et al. (2003) describe it as a cut-and-fill pattern that is associated with abrupt changes in channel direction during the migration process.

Sedimentological Model

The individual channels measured on seismic data are 200–300 m (656–984 ft) wide and 15–25 m (49–82 ft) thick. These channels stack up to form the lateral migration. The lithological composition observed on wireline logs and cored sections is fining and thinning upward. At its base, each channel is composed of coarse- to very coarse-grained sandstones, fining upward, to fine- to very fine-grained sandstones and laminated muddy turbidites to the top. Frequent slumped facies and sediment slides mass-transport complexes (MTCs) type Ia and Ib of Pickering and Corregidor (2005) can also be found within the lower part of the studied facies tract. These slumped facies and slide deposits, inducing a seismic lithological contrast, could correspond to the observed amplitude changes described by Kolla et al. (2001).

The vertical facies analysis, associated with observed seismic patterns, can lead to a process interpretation phase close to the Cronin et al. (2005) canyon infill hypothesis. The first phase corresponds to sediment bypass through the channel complex, inducing basal erosion of previously deposited sediments. Phase 2 is characterized by mixed erosion and deposition, with basal mass-transport complexes (type III) and local lag deposits. The destabilization of the channel border creates numerous small slump scars (MTCs type Ia and Ib), reflecting lateral wasting by slumping of channel margins toward the channel axes. High depositional topography and overbanking may cause slumping into the deep-water channels, causing flow blockage and consequent channel diversion (Imran et al., 1999). Phase 3 is a transition from sand to silt deposition in channel axes, just preceding the progressive abandonment of the system. Cronin et al. (2005) note the importance of mass-transport and slide deposits, which are not included in current models for slope-channel complexes. These produce mud pods within the canyon fill and probably also within individual channel fills.

According to Kolla and Perlmutter (1993), in channels connected to possible downstream canyons that are themselves connected to major fluvial systems, currents could be quasi–steady state or both steady and continuous and surge type (or catastrophic type). During sea level lowstands, the channel was possibly fed by a canyon, directly sourced by fluvial systems; both steady- and surge-type turbidity flows might have prevailed. During times of steady and continuous turbidity flows, deposition might occur more commonly on the convex (inner) side than on the concave (outer) side of the channel without any significant erosion (Imran et al., 1999).

The alternation of continuous and surge-type turbidity currents (Broucke et al., 2004), in addition to

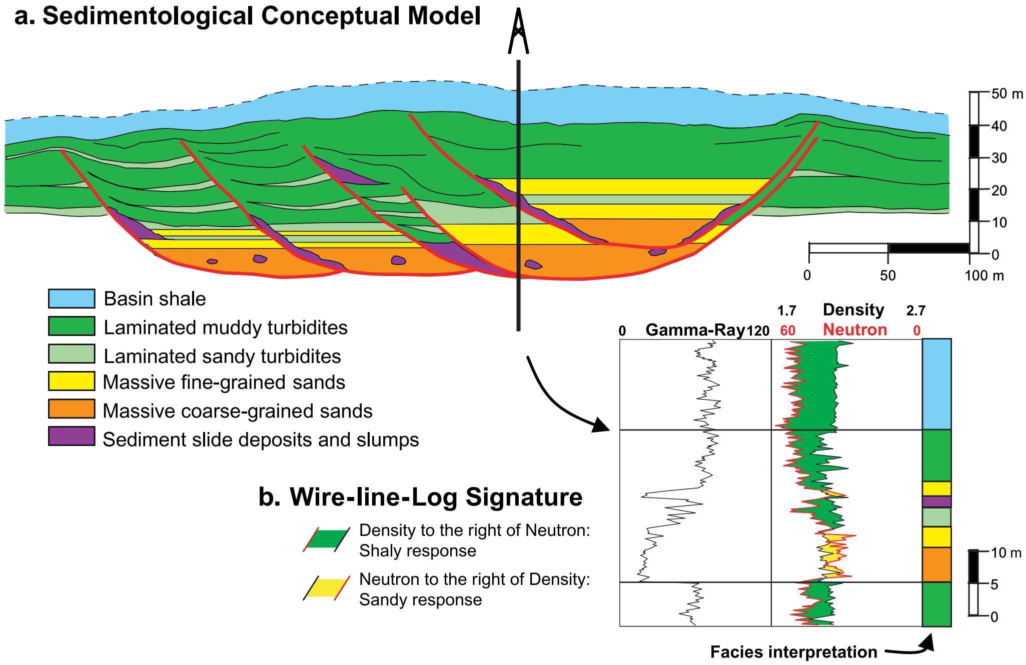

Figure 2. (a) Sedimentological conceptual model of the lateral migration pattern, obtained by successive cycles of erosion and construction of sinuous single channels migrating downdip as well as perpendicular to the flow direction (around 5 cycles). The migration is laterally unidirectional, and the channel migrates sideways, without reversing the lateral migration from one side to the other. The lateral migration and associated bypass through the channel lead to the erosion of the outer bend of the previously deposited elementary channel, thereby preserving most of the channel margin heterogeneities in the inner bend of the channel. These heterogeneities are composed of muddy sediment slides and slumps. The total unit is 500–1000 m (1640–3280 ft) wide and 15–25 m (49–82 ft) thick. (b) Typical wire-line-log signature observed in the lateral migration pattern. Wire-line-log signature is fining upward. A vertical penetration commonly encounters between 1 and 3 stacked elementary channels.

climatic and eustatic variations (Lopez, 2001; G. Turakiewicz, 2004, personal communication), leads to the formation of the overall lateral-migration architecture observed on seismic data (Figure 2). The channel complex results from successive erosion and construction cycles of sinuous, single channels migrating downdip as well as perpendicularly to flow direction. The oblique reflections observed on seismic cross sections could be associated with margin heterogeneities developed by slumping on the inner sides of the channels.

Two distinct channel-stacking organizations can be distinguished, with possible implications for reservoir characteristics, depending on whether fine-scale channel heterogeneities are preserved.

- Lateral-migration pattern (Figure 2): The migration is unidirectional, and the channel migrates sideways, without reversing the lateral migration from one side to the other. The total unit is 500–1000 m (1640–3280 ft) wide and 15–25 m (49–82 ft) thick. The wire-line-log signature is fining upward. A vertical penetration commonly encounters between one and three stacked elementary channels. The lateral migration and associated bypass through the channel lead to the erosion of the outer bend of the previously deposited elementary channel, thereby preserving most of the channel margin heterogeneities in the inner bend of the channel. These heterogeneities are composed of muddy sediment slides and slumps.
- Vertically stacked pattern (Figure 3): The sequence is the result of one or several episodes of channel sweep and swing. The total unit is 300–1000 m (984–3280 ft) wide and 25–30 m (82–98 ft) thick. The electrical log signature is cylindrical. A vertical penetration is encountered between three and five stacked elementary channels. Numerous internal erosions result in little likelihood of preservation of margin heterogeneities.

Considering the possible differences in terms of the preservation of fine-scale heterogeneity and, therefore, in petrophysical characteristics, two different sedimentological models are required.

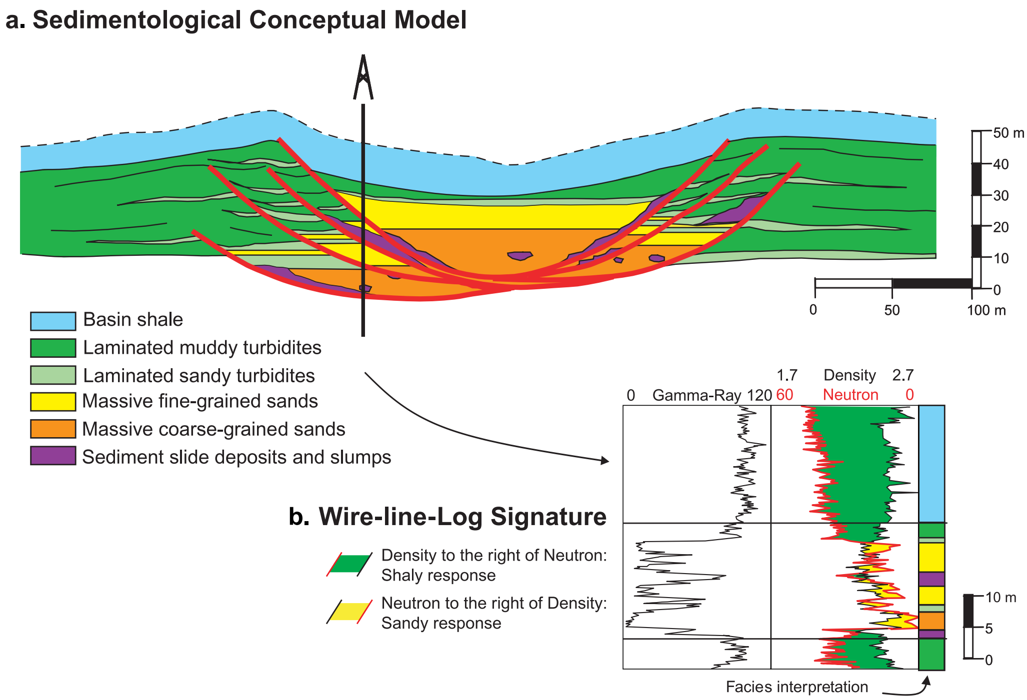

Figure 3. (a) Sedimentological conceptual model of the vertically stacked pattern, obtained by successive cycles of erosion and construction of sinuous single channels migrating downdip as well as perpendicular to the flow direction (around five cycles). This pattern results from one or more episodes of back-and-forth migration. Numerous internal erosions result in little likelihood of preservation of margin heterogeneities. The total unit is 300–1000 m (984–3280 ft) wide and 25–30 m (82–98 ft) thick. (b) Typical wire-line-log signature observed in the vertically stacked pattern. Electrical log signature is cylindrical. A vertical penetration encounters between three and five stacked elementary channels.

METHODOLOGY

The methodology developed in this study is a multistep workflow designed to create a geological reservoir model incorporating deterministic methods based on seismic data, well data, outcrop observations, sedimentological concepts, and analysis of geological uncertainties. This workflow integrates realistic geological and engineering attributes into the final numerical reservoir model, vital for optimal reservoir management (Pranter et al., 2005).

The modeling workflow is based on a small depth-converted extraction of the high-resolution seismic data, focusing on a specific area of the latest infill of the channel complex. This last filling stage is generally characterized by increasing sinuosity and developing lateral channel migration. The designated area is 3.2 km^2 (1.23 mi^2), calibrated by four wells, and is vertically limited by manually interpreted seismic horizons (base of the massive sands, top of the laminated sandy turbidites).

The modeling process is divided into three different steps. In the first step, individual channel envelopes based on seismic interpretation are defined deterministically. Following sedimentological concepts, these envelopes are then filled with turbidite facies identified in cored wells. This part of the modeling is divided into two processes. First, the facies are introduced deterministically. Second, to create mud pods (Cronin et al., 2005), an object-based modeling approach is overlaid onto the previous deterministic infill of individual channels. Finally, each model is filled with petrophysical characteristics using a stochastic workflow.

Deterministic Modeling of Channel Envelopes

The modeled region was separated into two distinct areas, the first showing a lateral migration of single channels and the second showing a vertically stacked pattern (Figure 4).

Fine-scaled models are built on the basis of a single architectural element: elementary channel. The successive phases of erosion mean that the true number of elementary channels is unknown. To achieve the widest possible range of architecture scenarios, this elementary body is reproduced between 5 and 10 times.

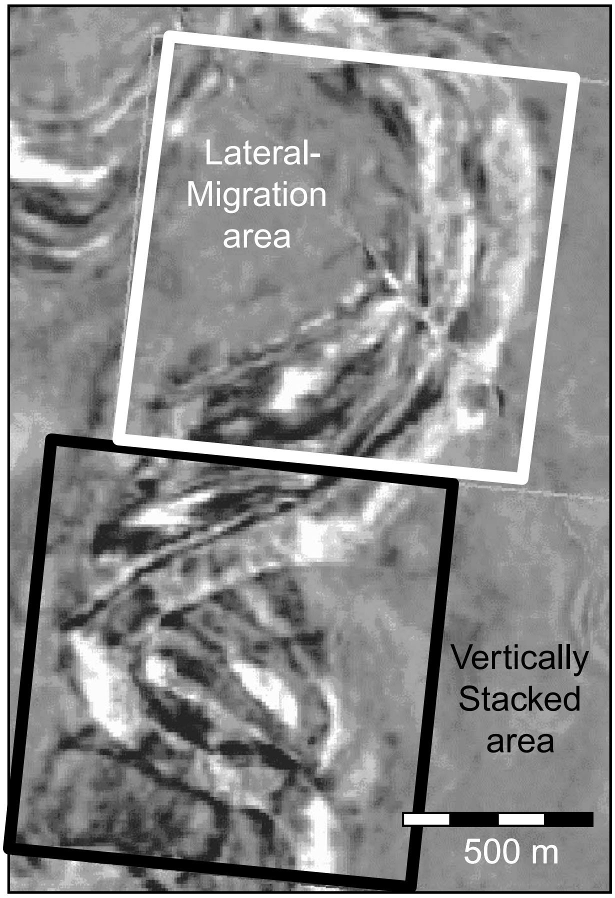

Figure 4. Selected modeling area for the two sedimentological patterns. Each model measures 1250 × 1250 × 70 m (4101 × 4101 × 229 ft).

The envelope for each single channel is constructed manually to respect seismic sections and map observations. Seismic data are used as guidelines to represent the morphology of the individual channels within the migration package as realistically as possible.

Forty depth-converted seismic sections were applied (Figure 5c). For each seismic section, every shingled reflection is interpreted (Figure 5a, approximately 10 reflectors). Each interpreted reflection, representing the preserved border of elementary channel, is artificially extended using symmetrical interpolations taken from the center of individual channels and aimed at restoring the morphology of elementary channels at deposition (Figure 5b). However, the individual morphology of elementary channels is known to be asymmetric (Abreu et al., 2003), and the resulting reconstructed borders will be eroded at the end of the modeling workflow.

Each channel envelope is reconstructed by a 3-D interpolation of its morphology. Stratigraphic grids are created for each elementary channel using interpolated surfaces.

In the final models, each channel is inserted in depositional order and erodes the underlying deposits (Figure 6).

The final models are orthogonal grids of 1250 m (4101 ft) in length by 1250 m (4101 ft) in width and 70 m (229 ft) in thickness, with cell sizes of 10 × 10 × 1 m (32 × 32 × 3.2 m).

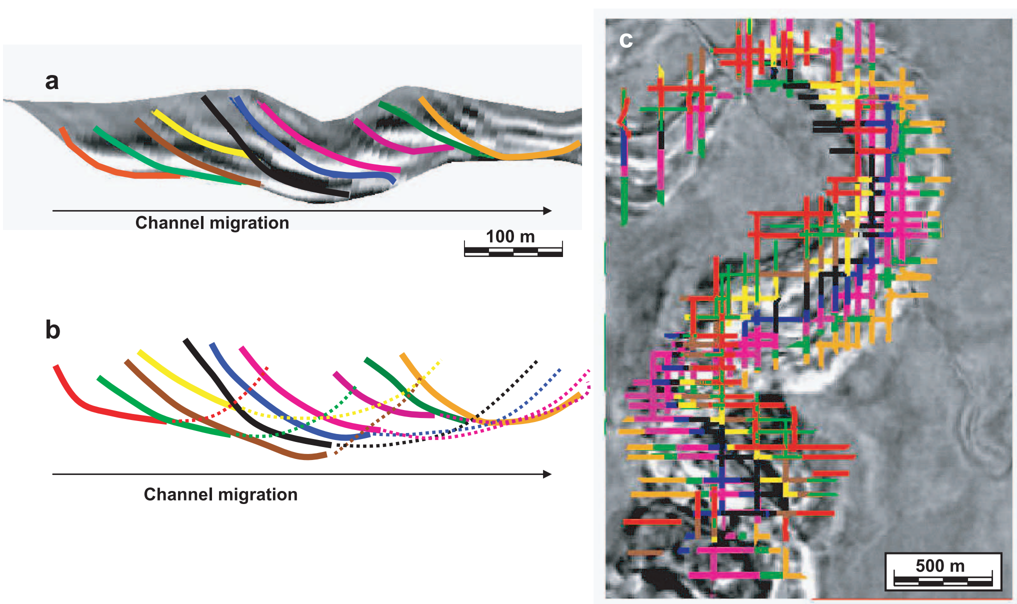

Figure 5. (a) Example of an interpreted depth-converted seismic section. (b) Restitution of channel morphology before erosion (dashed lines). (c) Position of the 40 depth-converted seismic sections used. Each channel is represented by a different color.

Figure 6. (a) Comparison between the amplitude time slice and (b) the result after inserting channels in depositional order. Channels are indicated with different colors to highlight the restitution of the overall morphology.

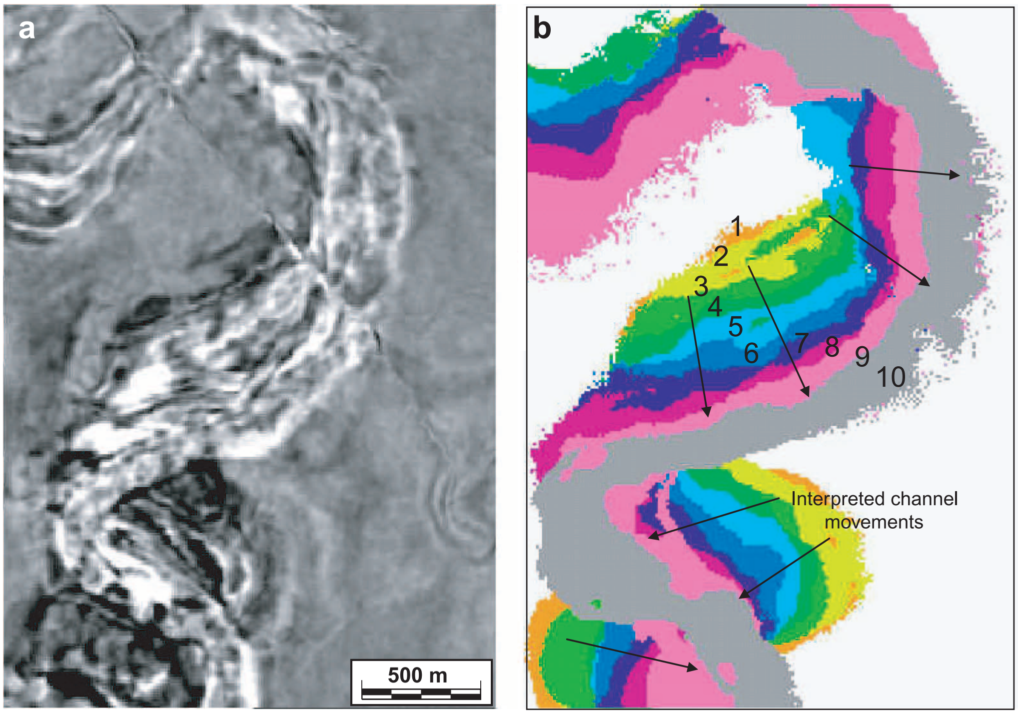

Channel Infill-Mixed Deterministic and Object-Based Approach

The filling of each single elementary channel is simplified to four facies associations with characteristics obtained from sedimentological interpretations of available wells.

The four facies associations are as follows.

- Basal channel fill consists of massive coarse-grained sandstones with a net sand content of between 70 and 85%. This represents two-thirds of the channel infill (6–10 m; 20–32 ft). Basal lag objects (gravel sands to conglomerates) may also be present at channel base. Basal channel fill is the first channel deposit following the initial erosion phase and is related to cohesive flow processes. The fill is composed of poorly sorted, coarse-grained sandstones with angular and rounded mud clasts and thereby has a permeability distribution ranging from 1 md to 1 d.
- Middle channel fill contains massive to cross-laminated, medium-grained sandstones grading upward to laminated, fine-grained turbidite sands with a net sand content of 80–90%. The mean thickness of channel-fill deposits is 4–5 m (13–16 ft). It is the depositional phase linked with a turbidite current decrease in velocity; the associated clean sandstones are generally well sorted and have permeability above 10 d.
- Abandonment deposits consist of fine intercalations of mud turbidites and ripple-laminated sands (tens-of-centimeter beds). The net sand content is between 40 and 70%. The mean thickness is 4–5 m (13–16 ft). Sand content linked to ripple-laminated beds associated with their well-sorted character leads to permeability values ranging from 100 md to 10 d; nevertheless, mud turbidite intercalations create a strong vertical anisotropy.
- Collapse margins are characterized by slide deposits and slumped laminated sandy to muddy turbidites. The overall net sand content is between 20 and 60%. The mean thickness of collapse-margin deposits is 2–6 m (6.5–20 ft). Collapse-margin deposits are caused by the destabilization of the channel border. They are composed of numerous small slump scars, which reflect lateral wasting of channel margins by slumping toward the channel axes. Because of their very low-permeability characteristics, they represent the main heterogeneities of elementary channel fills.

The spatial distribution of the main permeability barriers, composed of collapse-margin deposits, remains the major uncertainty for the sedimentological model. Some preliminary explanations of this distribution can be found on outcrop analogs (E. Remacha, 2002, personal communication; Young et al., 2003; Van Dyke et al., 2006; Slatt et al., in press) and actual observations

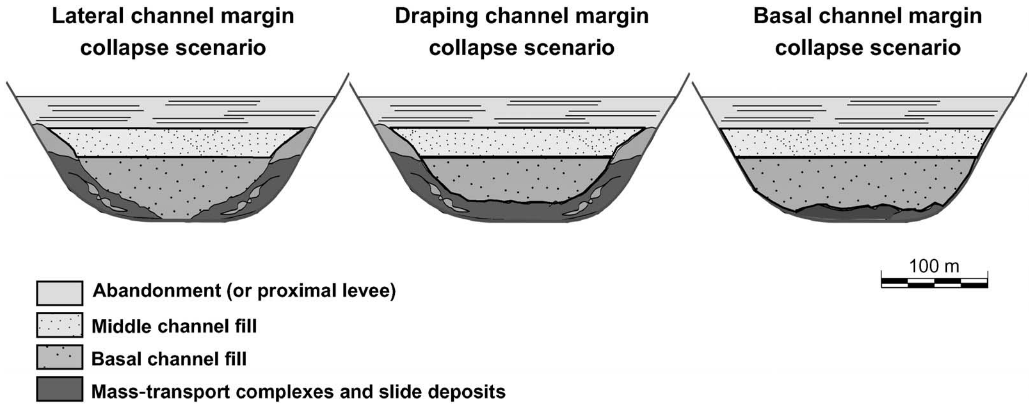

Figure 7. Schematic representation of the end members of elementary channel infill. The difference is caused by the distribution of channel margin collapse heterogeneities (a) lateral, (b) draping, or (c) basal.

(Cronin et al., 2005), but a discriminant distribution law cannot be applied.

To model a wide range of permeability barrier distribution and to integrate associated uncertainties, three distributions were modeled for each target area of interest (lateral migration and vertically stacked pattern). These scenarios represent end members of channel margin heterogeneity distribution encountered in this kind of depositional environment. The following are distinguished (Figure 7):

- Lateral channel margin collapse. The margin collapse deposits are present on the sides of the elementary channel; the heterogeneous facies is dominated by margin slide deposits.
- Draping channel margin collapse. The margin collapse deposits are present along the entire basal surface of the elementary channel, mixing basal mass-transport deposits and slide deposits.
- Basal channel margin collapse. The margin collapse deposits are present only at the base of the elementary channel, represented by axial mass-transport deposits.

Cross sections are built for each of these end-member scenarios. The interpolation of these cross sections along individual channels, using ''3-D discrete smooth interpolation'' (Mallet, 1989), provides a cube of facies occurrence. Horizontal and vertical facies proportions are extracted from each cross section. Vertical proportions are interpolated along the length of elementary channels to generate facies proportion maps. Horizontal proportions are assumed as homogeneous along the entire length of individual channels. This horizontal facies proportion is coupled with the previous proportion map to create a 3-D facies occurrence cube. A probability field simulation (Srivastava, 1992) using sequential Gaussian simulations and conditioned by the 3-D facies occurrence cube provides distributions of facies associations inside elementary channels. For each sedimentary scenario, the modeled permeability barriers are continuous (by distribution) along the entire length of the channel, although they are likely to be represented by pods distributed along the channels (Cronin et al., 2005). These pods are formed by lateral wasting of channel margins toward the channel axes by slumping (MTC types Ia and Ib) as well as by basal mass-transport complexes (type III). However, the real proportion of these pods is unknown.

Each sedimentary hypothesis is then degraded using geostatistic object-based modeling inside defined sedimentary regions (collapse deposits) to extend the heterogeneity distribution scenarios and to approach sedimentary reality. Mass-transport deposits and sediment slide, forming channel margin collapse deposits, are considered as a simple geometrical shape described by randomized parameters for orientation, length, width, and thickness (Dubrule et al., 1997). The dimensions applied for object simulations are extracted from core sedimentological analysis of the interval and conceptual models (Figure 8).

Object Dimensions (Collapse Deposits)

Length: minimum = 300 m (984 ft); mode = 500 m (1640 ft); maximum = 800 m (2624 ft).
Width: minimum = 20 m (65.6 ft); mode = 30 m (98.4 ft); maximum = 40 m (131.2 ft).
Thickness: minimum = 2 m (6.5 ft); mode = 4 m (13.1 ft); maximum = 6 m (19.7 ft).

For each sedimentological scenario (representing 100% of collapse deposits in defined areas: lateral, basal,

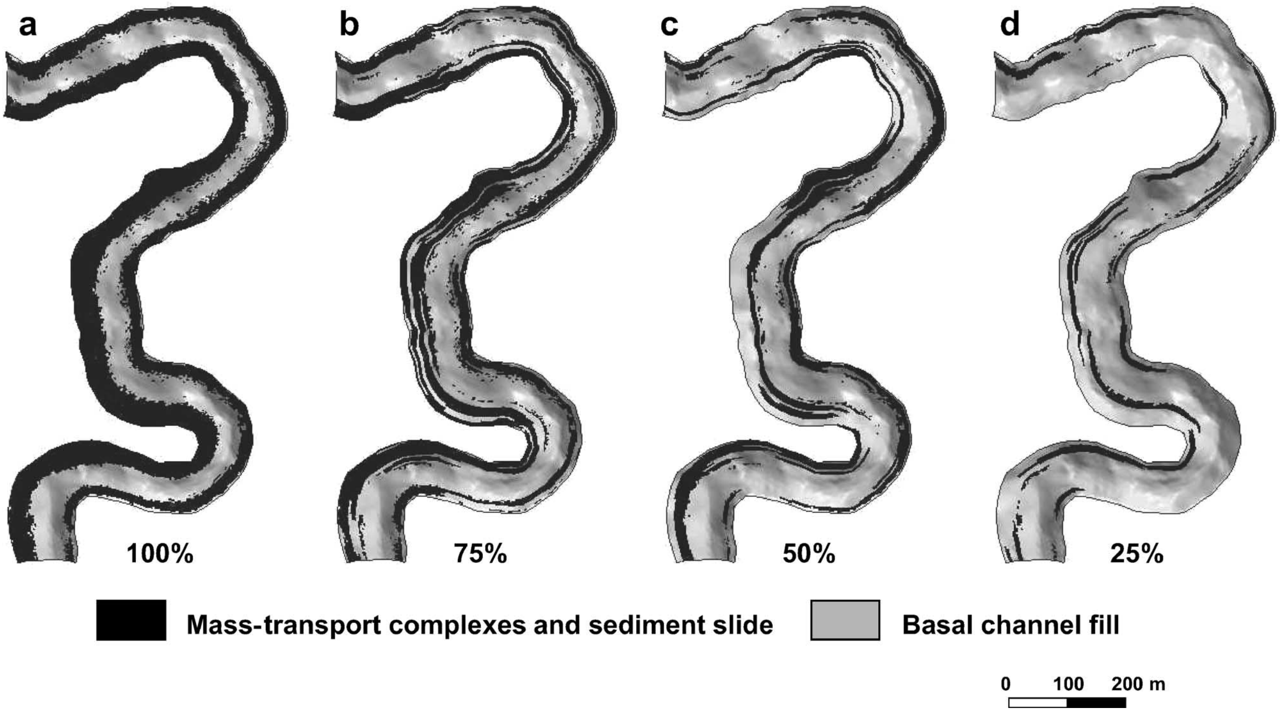

Figure 8. Object simulation applied to margin collapse deposits (example from lateral margin collapse sedimentological scenario). Collapse pods are obtained using object simulations. For each initial sedimentological scenario (representing 100% of collapse deposits), three more distributions of margin collapse deposits are generated of 25, 50, and 75% (example of a single object simulation in channel 1).

and draped), three more distributions of margin collapse deposits are generated: 25, 50, and 75%.

The object modeling workflow consists of several simulations to distribute the generated heterogeneities in random areas of elementary channels.

The final step of the modeling workflow (Figure 9) is stacking all the individual channels inside the two distinct final models (lateral migration and vertically stacked pattern). Because the real number of elementary channels in the migration complex is unknown, three assumptions are made to ascertain the impact this number might have on reservoir characteristics (10, 7, and 5 elementary channels). Each channel is inserted in depositional order and erodes underlying deposits. In

Figure 9. Construction of the 72 scenarios of heterogeneity distribution. Scenarios are built for the two sedimentological patterns (lateral migration and vertically stacked). For each pattern, three preliminary models are built with 10, 7, and 5 elementary channels (six models). The three end members of margin collapse distribution in elementary channels are then constructed for each selected model (18 models). Last, the degradation of margin collapse is added with selected proportions (72 models).

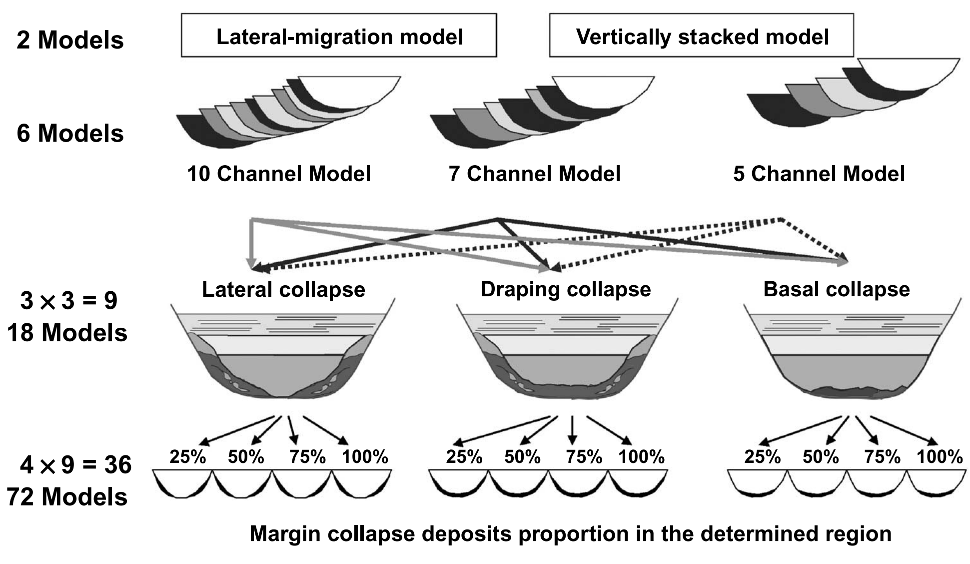

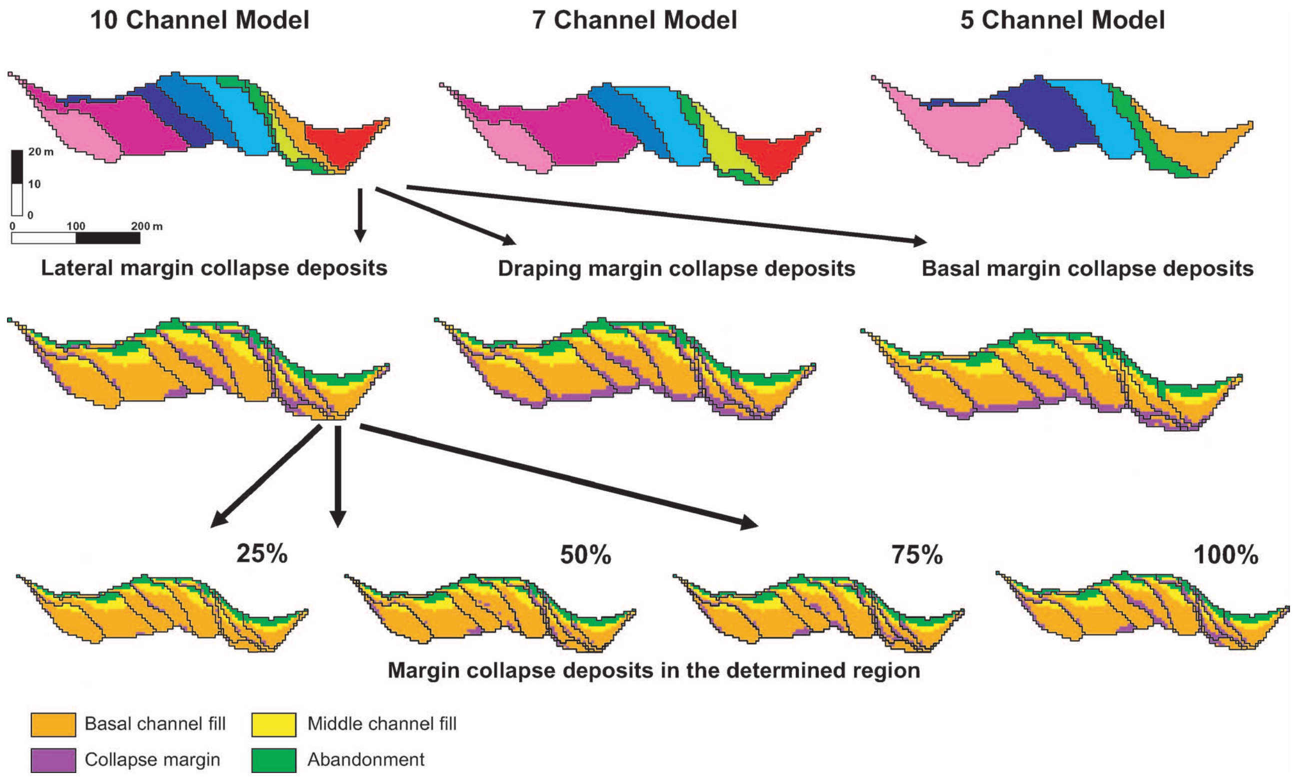

Figure 10. Visualization of each step of scenario creation on a cross section inside the lateral-migration model.

the end, 72 sedimentary scenarios of fine-scaled heterogeneity distributions are obtained inside the reservoir model (Figures 10, 11).

Petrophysical and Uncertainty Modeling

The findings of the previous deterministic sedimentological description are fed into a chain of tools to quantify subsurface uncertainties. This chain is composed of different softwares, each dealing with specific subsurface uncertainties (Corre et al., 2000).

The deterministic models are used as the construction framework for building several hundred equiprobable stochastic petrophysical models providing numerous reservoir images.

Each of the 72 sedimentological scenarios provides a consistent set of facies envelopes, within which several possible distributions of petrophysical properties can be generated. The simulations of the petrophysics in facies associations within each elementary channel are carried out using sequential Gaussian simulation (Deutsch and Journel, 1992).

A petrophysical data review derived from a selection of validated logs and core plugs was performed. This review was based on coding per facies associations at wells that encounter the geological object, which were then interpreted using in-house geostatistical software. Petrophysical distribution laws, vertical variograms, and correlation coefficients between variables were determined for each facies association (Figure 12). For each facies, net-to-gross, clay volume, porosity, and permeability distributions are defined. The most likely heterogeneity, to act as a barrier to intrareservoir fluid flow during production, is the poorer quality channel margin collapse facies (Young et al., 2003; Van Dyke et al., 2006; Weimer and Slatt, 2007). This deposit smears the contact surface between individual elementary channels. The magnitude of the permeability contrast between margin collapse deposits and the better quality basal channel fill and channel-fill sands (Figure 12) could result, locally, in poorly drained or totally bypassed areas.

A large number of geological reservoir models are simulated, and the corresponding volumes are calculated using a multistage (nested) simulation approach, which combines depositional facies and petrophysical parameter simulations. Uncertainties affecting geostatistical parameters, such as facies proportions, mean porosity, or variogram ranges, can also be incorporated. Resulting distributions can be visualized in 3-D, analyzed, and exported to a hydrocarbon flow simulator

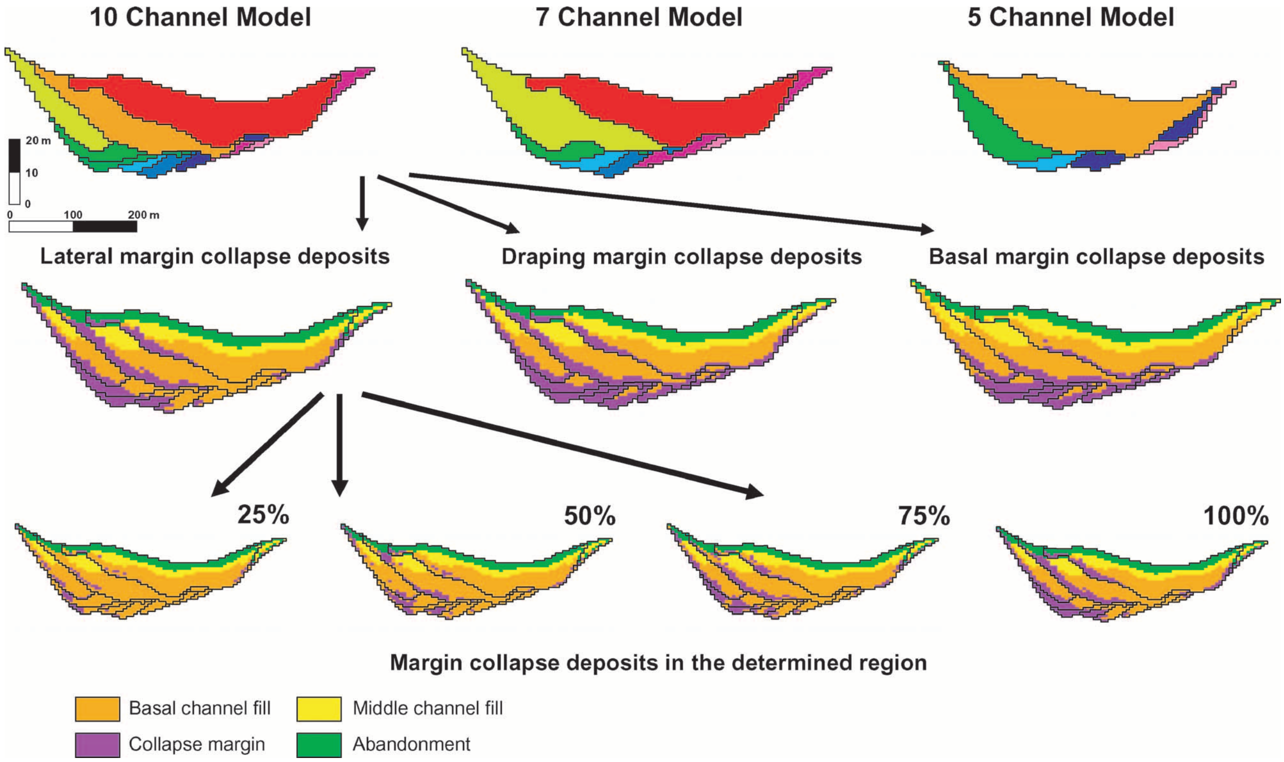

Figure 11. Visualization of each step of the scenario creation on a cross section inside the vertically stacked model.

Figure 12. Petrophysical property distribution derived from well logs and plug analysis. Margin collapse deposits (mass-transport and slide deposits) are clearly identified by petrophysical characteristics. They show (a) a high shale content; (b) low porosity; and (c) low permeability, whereas the other observed facies display similar distribution range for most of the petrophysical properties; (d) irreducible water saturation distributions.

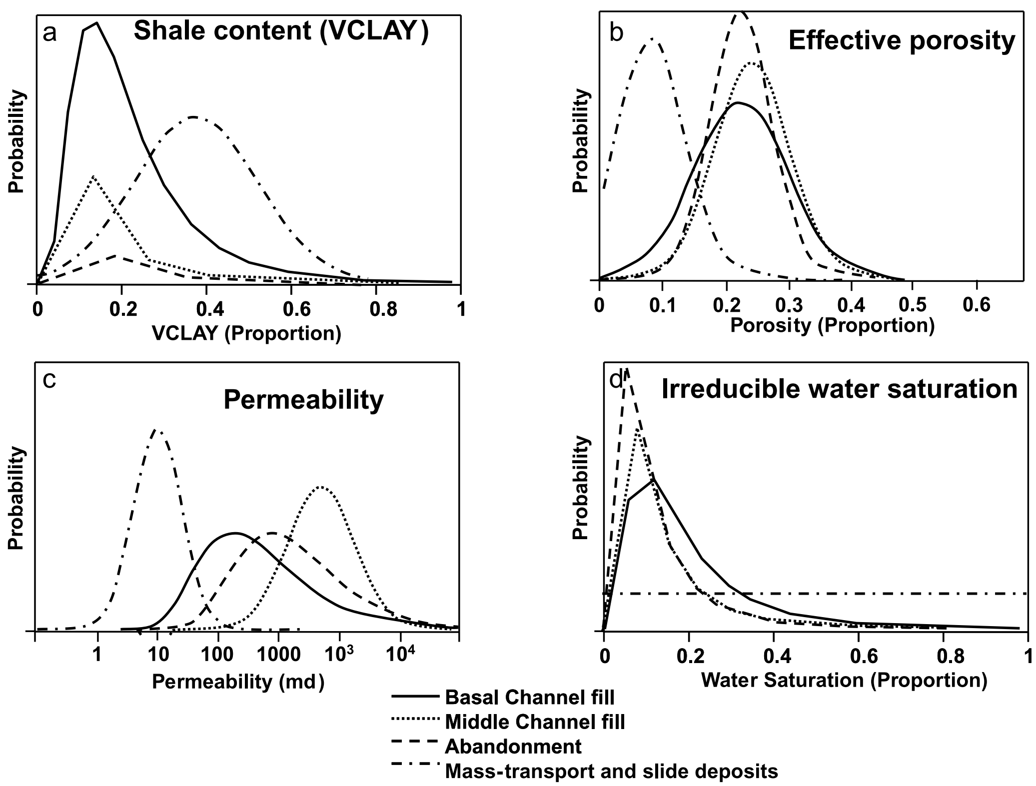

(Labourdette et al., 2006). At the end of the uncertainty workflow, a distribution of original oil in place is available for each scenario (Figure 13).

IMPACT ON STATIC CONNECTIVITY

Static connectivity to an injector-producer well pattern for each run result is automatically computed within the loop. To avoid direct connectivity problems and better appreciate the impact of lateral heterogeneity preservation between elementary channels, the model location of the injector and producer wells is designed, specifically, not to encounter the same elementary channels. Static connectivity is computed by applying a permeability threshold (0.1 md) to act as a communication cutoff in each model cell. It provides an idea of connectivity in the model prior to performing any dynamic simulation.

The resulting static connectivity can be plotted according to both initial sedimentary scenarios and the different margin collapse deposit proportions. The lateral-migration results are then compared with those from the vertically stacked pattern.

Figure 13 is a plot of normalized initial oil in place against normalized connected volumes. This static connectivity calculation shows a distinct separation of lateral-migration and vertically stacked patterns. Initial oil in place and static connected volumes are normalized according to each sedimentary pattern volume (cells filled with channel architectural element). The lateral-migration pattern shows connected oil volumes of between 50 and 70%; however, the vertically stacked pattern shows connected volumes of between 85 and 93%. The lower values of normalized oil in place for each pattern (left side of the plot) correspond to channels filled with fully draped mass-transport and slide deposits (100% of collapse-margin deposits). These emphasize the determinant impact of the lateral margin deposit proportions. This phenomenon can be observed in draped scenarios of the lateral-migration pattern (Figure 14). For this pattern, with the same sedimentological hypothesis, the variation in collapse-margin deposits can lead to a reduction of 8–15% of static connected volumes. In the vertically stacked pattern, these proportions seem to have a relatively low impact on static connected volumes, with a reduction of only between 2 and 4% of connected volume (Figure 15).

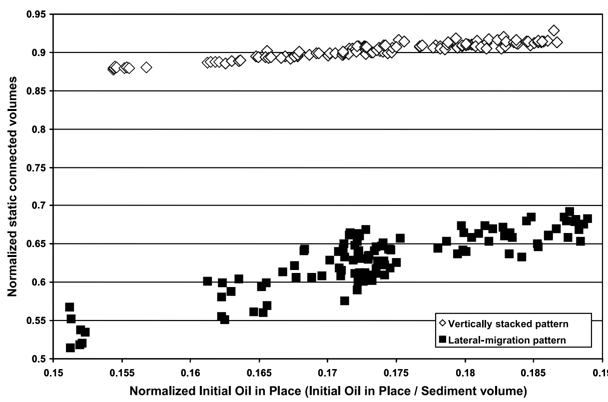

Figure 13. Normalized static connected volumes plotted against normalized connected oil in place volume (COIP). Initial oil-in-place and static connected volumes are normalized according to each sedimentary pattern volume (cells filled with channel architectural element). The lateral-migration pattern shows connected oil volumes between 50 and 70%, whereas the vertically stacked pattern shows connected volumes of between 85 and 93%.

Comparing the plots of Figures 14 and 15, we can observe the impact of the different initial sedimentological hypotheses. In the lateral-migration pattern, these hypotheses produce a gradational impact on connected volumes, from the drape-filled channels to basal-filled channels. This gradation is less evident in the vertically stacked pattern (Figure 15). The draped heterogeneities sedimentological hypothesis is most affected, but in a relatively minor way. These results indicate a different preservation rate of margin collapse heterogeneities between the lateral-migration pattern and the vertically stacked pattern. In the true lateral-migration pattern, margin heterogeneities are preserved, leading to a compartmentalization of the reservoir, particularly when margin collapse deposits drape the channel bases, thus acting as independent permeability conduits (Figure 14). In contrast, the vertically stacked pattern is not significantly influenced by any initial sedimentological scenarios nor by different collapse proportions (Figure 15). This is caused by the destruction of collapse baffles by the numerous crosscutting channel erosions.

CONCLUSIONS

This workflow integrates several different input data sets, ranging from seismic to well measurements and observations. It not only merges sedimentological concepts and observations using deterministic methods, but also introduces calibrated uncertainties using stochastic modeling.

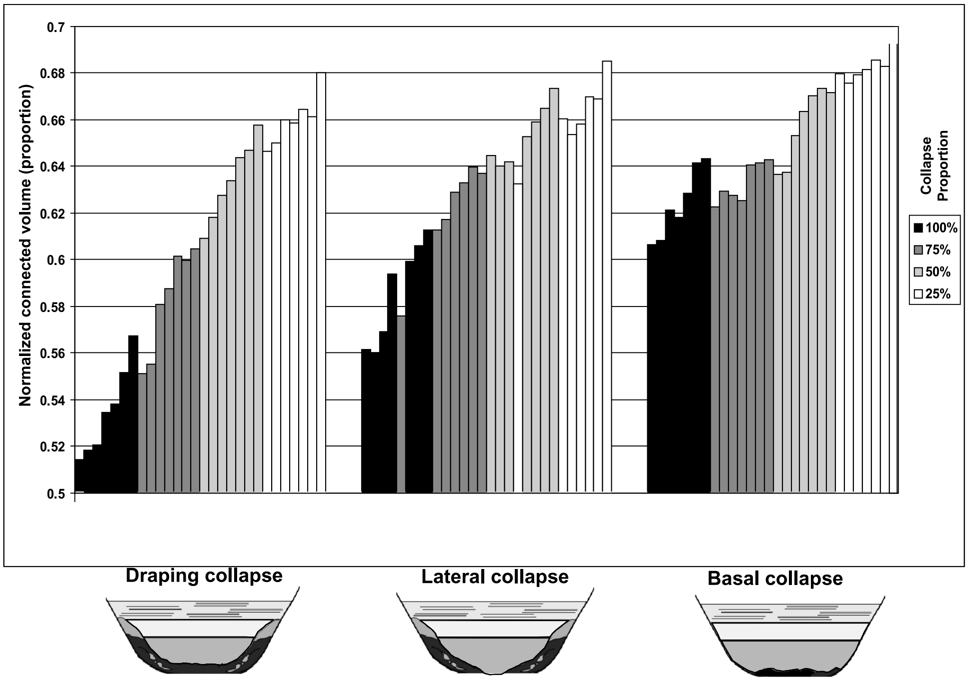

Figure 14. Normalized static connected volumes for the lateral-migration pattern, classified by sedimentological scenarios and sorted according to COIP and margin collapse proportions. Static connected volumes are directly related to collapse-margin proportions. The variation in collapse-margin deposits can lead to a reduction of 8–15% of static connected volumes.

This workflow is an integrated modeling approach, leading to the characterization of fine-scale heterogeneity and the quantification of its impact on reservoir properties. All types of recognized heterogeneity (sedimentological as well as petrophysical) were introduced into fine grid models. The static impact of these heterogeneities is highly dependent on channel migration patterns. Heterogeneities are mainly preserved in meander loops formed by lateral channel migration and act as independent permeability conduits. Inversely, vertically stacked patterns characterized by complex erosional patterns tend to decrease heterogeneity preservation, resulting in more reservoir connections. The degree of connectivity reflects the original proportion

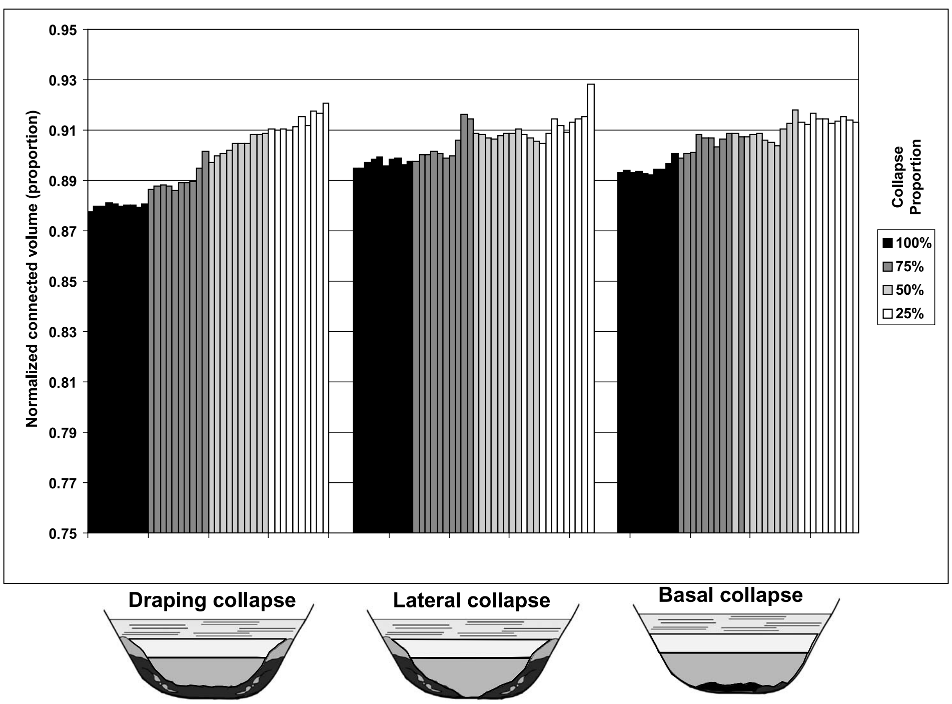

Figure 15. Normalized static connected volumes for the vertically stacked pattern, classified by sedimentological scenarios and sorted according to COIP and margin collapse proportions. Static connected volumes are not obviously related to collapse-margin proportions. The variation in collapse-margin deposits can lead to a reduction of only 2–4% of static connected volumes.

and distribution of the margin collapse facies as well as their preservation subsequent to channel switching and erosion. Using flow simulations in these models will result in a fluid-flow pattern focused more closely along individual channels in lateral-migration patterns (Labourdette et al., 2006). The lateral-migration pattern is identified as the last depositional element of channel complex infill and represents the highest uncertainty in hydrocarbon development potential. This is explained by the effect that subseismic sedimentological heterogeneities can have on production and reservoir management. Understanding the internal heterogeneity distribution and the dynamic impact these heterogeneities have on production is essential to optimize well designs and hydrocarbon recovery strategies, especially in stacked turbidite channel complexes.

REFERENCES CITED

Abreu, V., M. Sullivan, C. Pirmez, and D. Mohrig, 2003, Lateral accretion packages (LAPs): An important reservoir element in deep water sinuous channels: Marine and Petroleum Geology, v. 20, p. 631–648.

Arnott, R. W. C., 2005, Architecture of lateral accretion deposits in deep-marine sinuous channel fills (abs.): http://www.searchanddiscovery.com/documents/abstracts/2005annual_calgary/abstracts/arnott.

Beaubouef, R. T., 2004, Deep-water leveed-channel complexes of the Cerro Toro Formation, Upper Cretaceous, southern Chile: AAPG Bulletin, v. 88, p. 1471–1500.

Broucke, O., F. Temple, D. Rouby, C. Robin, S. Calassou, T. Nalpas, and F. Guillocheau, 2004, The role of deformation processes on the geometry of mud-dominated turbiditic systems, Oligocene and lower–middle Miocene of the lower Congo Basin (west African margin): Marine and Petroleum Geology, v. 21, p. 327–348.

Corre, B., P. Thore, V. de Feraudy, and G. Vincent, 2000, Integrated uncertainty assessment for project evaluation and risk analysis: Society of Petroleum Engineers European Conference, SPE Paper 65205, 9 p.

Coterill, K., S. K. Dholakia, J. Coleman, A. Champagne, D. Marotta, M. Pasley, G. Tari, L. Binga, and H. Van Dierendock, 1999, Sinuous morphologies in submarine channels— Scale and geometries in seismic and outcrop indicating possible mechanisms for deposition (abs.): UK99, AAPG International Conference and Exhibition, p. 136–138.

Cronin, B. T., 1995, Structurally controlled deep-sea channel courses: Examples from the Miocene of southeast Spain and the Alboran Sea, southwest Mediterranean, *in* A. J. Hartley and D. J. Prosser, eds., Characterization of deep marine clastic systems: Geological Society (London) Special Publication 94, p. 113–133.

Cronin, B. T., A. M. Akhmetzhanov, A. Mazzini, G. Akhmanov, M. Ivanov, and N. H. Kenyon, 2005, Morphology, evolution and fill: Implications for sand and mud distribution in filling deep-water canyons and slope channel complexes: Sedimentary Geology, v. 179, p. 71–97.

Da Costa, J. L., T. W. Schirmer, and B. R. Laws, 2001, Lower Congo Basin, deep-water exploration province, offshore west Africa, *in* J. C. Threet and W. A. Morgan, eds., Petroleum provinces of the twenty-first century: AAPG Memoir 74, p. 517–530.

Damuth, J. E., V. Kolla, R. D. Flood, R. O. Kowsmann, M. C. Monteiro, M. A. Gorini, J. J. C. Palma, and R. H. Belderson, 1983, Distributary channel meandering and bifurcation patterns on the Amazon deep-sea fan as revealed by long-range side-scan sonar (GLORIA): Geology, v. 11, p. 94–98.

Damuth, J. E., R. D. Flood, R. O. Kowsmann, R. H. Belderson, and M. A. Gorini, 1988, Anatomy and growth pattern of Amazon deep-sea fan as revealed by long-range side-scan sonar (GLORIA) and high-resolution seismic studies: AAPG Bulletin, v. 72, p. 885–911.

Deutsch, C. V., and A. G. Journel, 1992, GSLIB: Geostatistical software library and user's guide: New York, Oxford University Press, 340 p.

Dubrule, O., C. Basire, S. Bombarde, P. Samson, D. Segonds, and J. Wonham, 1997, Reservoir geology using 3-D modelling tools: Society of Petroleum Engineers Annual Technical Conference and Exhibition, San Antonio, Texas, SPE Paper 38659, 16 p.

Elliott, T., 2000, Depositional architecture of a sand-rich, channelized turbidite system: The Upper Carboniferous Ross Sandstone Formation, western Ireland: Gulf Coast Section SEPM Foundation 20th Annual Research Conference, Deep-Water Reservoirs of the World, p. 342–373.

Garrison, L. E., N. H. Kenyon, and A. H. Bouma, 1982, Channel systems and lobe construction in the Mississippi Fan: Geo-Marine Letters, v. 2, p. 31–39.

Hurst, A., B. T. Cronin, and A. J. Hartley, 2000, Reservoir modelling sand-rich deep water clastics: The necessity of down-scaling: Petroleum Geoscience, v. 6, p. 67–76.

Imran, J., G. Parker, and C. Pirmez, 1999, A nonlinear model of flow in meandering submarine and subaerial channels: Journal of Fluid Mechanics, v. 400, p. 295–331.

Kastens, K. A., and A. N. Shor, 1985, Depositional processes of a meandering channel on Mississippi Fan: AAPG Bulletin, v. 69, p. 190–202.

Kolla, V., and F. Coumes, 1987, Morphology, internal structure, seismic stratigraphy, and sedimentation of Indus Fan: AAPG Bulletin, v. 71, p. 650–677.

Kolla, V., and M. A. Perlmutter, 1993, Timing of turbidite sedimentation on the Mississippi Fan: AAPG Bulletin, v. 77, p. 1129–1141.

Kolla, V., P. Bourges, J.-M. Urruty, D. Claude, M. Morice, J. Durand, and N. H. Kenyon, 1998, Reservoir architecture in recent and subsurface deep-water meander channel and related depositional forms (abs.): European Association of Geoscientists and Engineers/AAPG Third Research Symposium Extended Abstracts, 1 p.

Kolla, V., P. Bourges, J. M. Urruty, and P. Safa, 2001, Evolution of deep-water Tertiary sinuous channels offshore Angola (west Africa) and implications for reservoir architecture: AAPG Bulletin, v. 85, p. 1373–1405.

Labourdette, R., J. Poncet, J. Seguin, F. Temple, J. Hegre, and A. Irving, 2006, Three-dimensional modelling of stacked turbidite channels in west Africa: Impact on dynamic reservoir simulations: Petroleum Geoscience, v. 12, p. 335–345.

Lopez, M., 2001, Architecture and depositional pattern of the Quaternary deep-sea fan of the Amazon: Marine and Petroleum Geology, v. 18, p. 479–486.

Mallet, J.-L., 1989, Discrete smooth interpolation in geometric modeling: Association for Computing Machinery Transactions on Graphics, v. 8, p. 121–144.

Martinsen, O. J., T. Lien, and R. G. Walker, 2000, Upper Carboniferous deep water sediments, western Ireland analogues for passive margin turbidite plays: Gulf Coast Section SEPM Foundation 20th Annual Research Conference, Deep-Water Reservoirs of the World, p. 533–555.

Mayall, M., and C. J. O'Byrne, 2002, Reservoir prediction and development challenges in turbidite slope channels: Offshore Technology Conference, OTC Paper 14029, 10 p.

Mayall, M., and I. Stewart, 2000, The architecture of turbidite slope channel: Gulf Coast Section SEPM Foundation 20th Annual Research Conference, Deep-Water Reservoirs of the World, p. 578–586.

Menard, H. W., 1955, Deep-sea channels, topography, and sedimentation: AAPG Bulletin, v. 39, p. 236–255.

Mutti, E., and W. R. Normark, 1991, An integrated approach to the study of turbidite systems, *in* P. Weimer and M. H. Link, eds., Seismic facies and sedimentary processes of submarine fans and turbidite systems: Frontiers in sedimentary geology: New York, Springer-Verlag, p. 75–106.

Nelson, J. M., and J. D. Smith, 1989, Flow in meandering channels with natural topography, *in* S. Ikeda and G. Parker, eds., River meandering: Water Resource Monographs, v. 12, p. 69–102.

Peakall, J., B. McCaffrey, and B. Kneller, 2000, A process model for the evolution, morphology, and architecture of sinuous submarine channels: Journal of Sedimentary Research, v. 70, p. 434–448.

Pickering, K. T., and J. Corregidor, 2005, Mass-transport complexes (MTCs) and tectonic control on basin-floor submarine fans, middle Eocene, south Spanish Pyrenees: Journal of Sedimentary Research, v. 75, p. 761–783.

Posamentier, H. W., and V. Kolla, 2003, Seismic geomorphology and stratigraphy of depositional elements in deep-water settings: Journal of Sedimentary Research, v. 73, p. 367–388.

Pranter, M. J., A. R. Zulfiquar, and P. Weimer, 2005, A novel integrated approach to stochastic deep-water reservoir modelling using sequence-stratigraphic and geomorphic constraints (abs.): AAPG Annual Meeting Program, v. 89, 1 p.

Prather, B. E., F. B. Keller, and M. A. Chapin, 2000, Hierarchy of deep water architectural elements with reference to seismic resolution: Implications for reservoir prediction: Gulf Coast Section SEPM Foundation 20th Annual Research Conference, Deep-Water Reservoirs of the World, p. 817–835.

Roberts, M. T., and B. Compani, 1996, Miocene example of a meandering submarine channel-levee system from 3D seismic reflection data, Gulf of Mexico Basin: Gulf Coast Section SEPM Foundation, 17th Annual Research Conference, p. 241–254.

Saller, A. H., J. T. Noah, A. P. Ruzuar, and R. Schneider, 2004, Linked lowstand delta to basin-floor fan deposition, offshore Indonesia: An analog for deep-water reservoir systems: AAPG Bulletin, v. 88, p. 21–46.

Skene, K. I., D. J. W. Piper, and P. S. Hill, 2002, Quantitative analysis of variations in depositional sequence thickness from submarine channel levees: Sedimentology, v. 49, p. 1411–1430.

Slatt, R. M., J. Minken, S. K. Van Dyke, D. R. Pyles, A. J. Witten, and R. A. Young, in press, Scales of heterogeneity of an outcropping leveed-channel system, Cretaceous Dad Sandstone Member, Lewis Shale, Wyoming, U.S.A., *in* T. H. Nilsen, R. D. Shew, G. S. Steffens, and J. R. J. Studlick, eds., Atlas of deepwater outcrops: AAPG Studies in Geology 56.

Srivastava, R. M., 1992, Reservoir characterization with probability field simulation: Society of Petroleum Engineers Annual Technical Conference and Exhibition, SPE Paper 24753, 12 p.

Stelting, C. E., et al., 1985, Migratory characteristics of mid-fan meander belt, Mississippi Fan, *in* A. H. Bouma, W. R. Normark, and N. E. Barnes, eds., Submarine fans and related turbidite systems: New York, Springer-Verlag, p. 283–290.

Stephens, A. R., G. D. Monson, and J. M. Reilly, 1996, The relevance of seismic amplitudes in exploring the Niger Delta: Offshore West Africa Conference Papers, v. 56, p. 54–60.

Stright, L., J. Caers, H. Li, F. Van Der Vlugt, C. Pirmez, and M. Barton, 2006, Modeling, upscaling and history matching thin, irregularly-shaped flow barriers: A comprehensive approach for predicting reservoir connectivity: 26th Annual Gulf Coast Section SEPM Foundation Bob F. Perkins Research Conference—Reservoir Characterization: Integrating Technology and Business Practices, p. 985–1002.

Temple, F., and O. Broucke, 2004, Sedimentological models of the Oligocene and Miocene Malembo Formation in offshore Angola (lower Congo Basin): Regional West African Deepwater Conference and Exhibition, Abuja, Nigeria: AAPG Bulletin, v. 88, 1 p.

Tomasso, M., F. L. Bonnafé, R. Bouroullec, D. R. Pyles, and D. C. Jennette, 2006, Outcrop versus seismic architecture of deepwater deposits: Use of LiDAR along the slope-to-basin transect of the Brushy Canyon Formation, west Texas: 26th Annual Gulf Coast Section SEPM Foundation Bob F. Perkins Research Conference— Reservoir Characterization: Integrating Technology and Business Practices, p. 755–770.

Van Dyke, S. K., R. M. Slatt, J. Dodson, C. Valerio, N. Buckner, H. Correa-correa, and B. Ojo, 2006, High frequency characterization of an outcropping, sinuous leveed-channel complex, Dad Sandstone Member, Lewis Shale, Wyoming: 26th Annual Gulf Coast Section SEPM Foundation Bob F. Perkins Research Conference— Reservoir Characterization: Integrating Technology and Business Practices, p. 771–812.

Weimer, P., and R. M. Slatt, 2007, Petroleum geology of deepwater settings: AAPG Studies in Geology 57, 816 p.

Weimer, P., R. M. Slatt, P. Dromgoole, M. Bowman, and A. Leonard, 2000, Developing and managing turbidite reservoirs: Case histories and experiences: Results of the 1998 European Association of Geoscientists and Engineers/AAPG Research Conference: AAPG Bulletin, v. 84, p. 453–465.

Young, R. A., R. M. Slatt, and J. G. Staggs, 2003, Application of ground penetrating radar imaging to deepwater (turbidite) outcrops: Marine and Petroleum Geology, v. 20, p. 809–821.